DOE/NASA/3303-1
NASA CR-168108
M.I.T. ASRL TR 197-2

Some Experiments on Yaw Stability of Wind Turbines with Various Coning Angles

David Bundas and John Dugundji
Massachusetts Institute of Technology

July 1981

Prepared for
NATIONAL AERONAUTICS AND SPACE ADMINISTRATION
Lewis Research Center
Under Grant NSG-3303

for
U.S. DEPARTMENT OF ENERGY
Conservation and Renewable Energy
Division of Photovoltaic Energy Technology

DOE/NASA/3303-1
NASA CR-168108
M.I.T. ASRL TR 197-2

Some Experiments on Yaw Stability of Wind Turbines with Various Coning Angles

David Bundas and John Dugundji
Aeroelastic and Structures Research Laboratory
Massachusetts Institute of Technology
Cambridge, Massachusetts 02139

July 1981

Prepared for
National Aeronautics and Space Administration
Lewis Research Center
Cleveland, Ohio 44135
Under Grant NSG-3303

for
U.S. DEPARTMENT OF ENERGY
Conservation and Renewable Energy
Division of Photovoltaic Energy Technology
Washington, D.C. 20545
Under Interagency Agreement DE-AI01-76ET20320

TABLE OF CONTENTS

SECTION 1
INTRODUCTION

A wind turbine which aligns itself with the wind is more efficient than one which is mechanically aligned. To study the effect of coning angle on yawing moments, a small model was constructed with variable pitch and coning angles. Coning angle β is defined as the angle the blades make with the perpendicular to the wind turbine's shaft axis, while yaw angle α_y is the angle between the wind turbine shaft and the wind direction. See Fig. 1.

For a given change in yaw angle a moment is produced. Depending on the wind turbine configuration, it will tend to either position the wind turbine into the wind (stable configuration), or turn it out of the wind (unstable configuration). A simple theory for this yaw behavior has been presented by Miller in Ref. 1.

The wind turbine model used here was set up in a wind tunnel and aligned with the wind. As it was turned out of the wind, readings of the yaw moment and angular frequency of the blades were recorded. These readings were compared with the simple theory. As a qualitative check, the restraining bar was removed and the wind turbine was allowed to pivot freely, verifying quantitative data.

This experiment was a continuation of work begun in the M.I.T. Course 16.62, Experimental Projects Lab, with Laura Rodman as a co-worker. The wind turbine model constructed at that time was used, with some modification, for this experiment.

SECTION 2
EXPERIMENT

2.1 Apparatus

The general setup showing wind turbine and turntable in the wind tunnel is shown in Fig. 2. The freely privoting wind turbine was constructed to allow for variable coning and pitch angles. Shown in Fig. 3 is the body of the wind turbine without the nacelle. The wind turbine blades were free to rotate, slowed only by the wind drag and the friction in the bearings.

Each of the wind turbine blades was constructed of a piece of mahogony. A jointer blade was ground down to the airfoil shape and the mahogony was run through the machine. The resulting blade had a length of 25.4 cm (10 in) and a chord of 3.81 cm (1.5 in). The asymmetric airfoil was 15% thick at quarter chord, and the blade did not have any twist. For added strength a steel spar was epoxied into a slot cut in the airfoil at about the quarter chord point. Welded to the steel bar was a threaded bolt. The blade angle of attack for the tests was set at 7°.

Tests were made to see if the blades could hold up to expected centrifugal and drag loads. Centrifugal loads become important in the bending of blades set at a coning angle. The blades were designed to operate at 2000 rpm with a factor of safety of two.

Two hubs were constructed, one for ±10°, and one for 0° coning angle. The hubs are two blocks of aluminum bolted together. At each end there is a threaded hole into which the blade is screwed. On one hub these, holes were drilled at 10°, and on the other hub they were drilled at 0°. The bolt on

the blades was attached there, and by tightening the eight bolts that hold the two pieces of the hub together, one can hold the blades at any desired pitch angle. As shown in Fig. 3, the hub was held to the shaft by two set screws.

Measuring devices are shown in Fig. 4. To measure yawing moments, a restraining bar was clamped in the stationary tower, and clamped between two set screws on the wind turbine. Strain gauges attached to the bar were read through a chart recorder. By calibrating the chart recorder, a continuous readout of the yawing moment was produced. A readout proportional to the moment could also be read on a volt-meter.

A photoelectric switch was used to measure the angular frequency of the blades. A cardboard disk attached to the shaft with a slot cut in it was used to generate pulses from the switch as it rotated. The signal from the switch was amplified, and a readout of the period of revolution was obtained fron a counter.

Tests were conducted in the 5 foot x 7 foot Acoustic Wind Tunnel at M.I.T., which produced a uniform wind speed at the test section. A turntable was constructed to allow for any yaw angle setting of the wind turbine.

2.2 Testing Procedure

The wind turbine was placed in the wind tunnel, and the moment readout was calibrated by applying known weights on a known torque arm. The wind turbine was set to 0° yaw angle and the tunnel brought up to speed. The windspeed for all the tests was 4.53 m/sec (14.9 ft/sec), and the blade angle was set at a constant pitch angle of 7°. This produced a rotational frequency of about 19 Hz, or 1140 rpm. Readings of yawing moment and rotational frequency

were taken. Next, the wind turbine was moved to a yaw angle of 5° with the wind still on. Readings were taken here and at every 5° until the wind turbine stopped rotating. This procedure was followed for both the upwind and downwind cases at both $\pm 10°$ and 0° yaw angle. The blades were also removed from the model and the nacelle alone was tested to determine what moment it produced in the wind.

Later, the restraining bar was removed, and qualitative tests of the now freely yawing wind turbine were also performed in the wind tunnel.

SECTION 3

RESULTS AND DISCUSSION

Plots of yawing moment versus yaw angle are shown in Figs. 5 to 10 for each configuration tested. Negative slopes of $dC_M/d\alpha$ indicate stable yaw behavior, while positive slopes indicate instability. The dashed line in these figures represents the value obtained when nacelle effects are subtracted. Nacelle effects can be dealt with in this way because the wind turbine took very little power from the wind. The graph of yawing moment versus yaw angle for the nacelle alone is shown in Fig. 11.

The variation of rotational frequency of the blades Ω with yaw angle α_y is shown in Fig. 12. The drop-off of rotational frequency with angle of yaw is generally the same for all cases, except perhaps for the $\beta = +10°$ cases where the drop-off is somewhat less. The drop-off seems to follow roughly a cosine curve variation as indicated in the figure. Beyond a yaw angle of about 50°, the wind turbine would stop spinning.

The yaw moment characteristics given in Figs. 5-10 were compared with the simple theory presented by Miller in Ref. 1. There, assuming ideally twisted blades and simple blade element theory, the yaw stability characteristics at zero angle of yaw are determined as,

$$\frac{dM}{d\alpha_y} = \frac{n\,\rho\,a\,c\,\Omega\,R^3 V}{4}\left[\frac{\beta}{3} + \frac{\ell}{R}\left(\frac{C_{Do}}{a} + \lambda\,\theta_o + \frac{\beta^2}{2}\right)\right] \tag{1}$$

where one has,

n = number of blades

ρ = air density

a = lift curve slope

c = chord

Ω = rotation speed

R = blade radius

V = wind speed

β = coning angle

ℓ = length between yaw pivot and hub

C_{Do} = drag coefficient

θ_o = blade tip angle for ideal twist.

and the directions of positive moments, angles, etc. are shown in Fig. 1. The above expression can be nondimensionalized by introducing the yaw moment coefficient C_M and the blade solidity ratio σ defined as,

$$C_M = M \Big/ \frac{1}{2} \rho V^2 \pi R^3 \tag{2}$$

$$\sigma = \frac{\text{Blade area}}{\text{Disk area}} = \frac{nc}{\pi R} \tag{3}$$

This gives the simple yaw moment stability derivative from Ref. 1 as,

$$\frac{dC_M}{d\alpha_y} = \sigma \frac{a}{2} \frac{\Omega R}{V} \left[\frac{\beta}{3} + \frac{\ell}{R} \left(\frac{C_{Do}}{a} + \lambda \theta_o + \frac{\beta^2}{2} \right) \right] \tag{4}$$

The parameters for the present wind turbine are given in Appendix A, assuming equivalently ideally twisted blades, $\theta = \theta_0 R/r$. Placing these into Eq. (4) gives the theoretical results shown in Table 1. Comparing these with the experimental results of Figs. 5-10, it is seen that the trends are the same, i.e., going from positive to negative coning increases the stability, and the downward cases are more stable than the upwind cases. However, all experimental cases were found to be stable for small angles of yaw, whereas the simple theory indicated the $\beta = +10°$ cases would be unstable. The poor numerical correlation is possibly due to stalling effects of the untwisted blades used here.

When the wind turbine was allowed to pivot freely the experimental static data was confirmed. All cases were stable when spinning at the equilibrium, free-wheeling rotation speed, with the most stable case from the previous static data being the most stable qualitatively. Configurations for which unstable data was taken moved out of the wind for a large enough yaw angle, then slowed down and stopped.*

Although all cases were stable at the equilibrium speed, all cases were unstable at some lower rotational speed while they were spinning up. None of the configurations would self start and the wind turbine had to be held to be started. The previously mentioned ranking of stability holds here as well. The most stable becomes stable at a lower rotational speed than the next most stable, etc.

*The neutral position for the nacelle when the blades had stopped was perpendicular to the wind.

SECTION 4

CONCLUSIONS

Yaw moments produced by a spinning wind turbine were measured experimentally and seen to be stable for coning angles of +10°, 0°, -10° in both the upwind and downwind configurations. These results were obtained for a given wind spped, with rotors operating at high rotation speeds corresponding to the free-wheeling, no power condition. At lower rotation speeds where the blades were spinning up (high blade angles of attack), all the configurations were unstable and if free, the turbine would yaw out of the wind. This prevented the turbine from spinning up, unless it was held locked into the wind.

Correlation of the experimental data with the simple theory of Ref. 1 is poor, possibly due to stalling effects of the untwisted blades used here. However, the experimental trend for the effect of coning corresponded to the simple theory, i.e., rotors coned away from the wind were more stable than those coned into the wind.

The above yaw results may be of interest in the operation of horizontal axis wind turbines during start-up and wind gusting conditions.

APPENDIX A

WIND TURBINE PARAMETERS

For the present, constant blade pitch wind turbine, the following parameters were measured or assumed,

$$n = 2$$

$$\rho = 1.22 \ \ Kg/m^3 = .00238 \ \ slugs/ft^3$$

$$a = 5.5$$

$$c = .0381 \ \ m = 1.5 \ in$$

$$\Omega = 19 \ \ Hz = 119.4 \ rad/sec$$

$$R = .305 \ m \ \ \ m = 1 \ ft$$

$$V = 4.54 \ m/sec = 14.9 \ \ ft/sec$$

$$\beta = 10° = .1745 \ \ rad$$

$$\ell = .0519 \ m = 3.5 \ in$$

$$r_N = .0554 \ m = 2.15 \ in$$

$$\theta = 7° \ \ = .1222 \ rad$$

Matching the constant pitch blade to an ideally twisted rotor $\theta = \theta_o \, R/r$ at 75% radius gives the equivalent pitch angle,

$$\theta_o = .75 \ (7°) = 5.25° = .0916 \ rad$$

Also, one obtains the tip speed and solidity ratios as

$$\frac{\Omega R}{V} = \frac{119.4\ (.305)}{4.54} = 8.02$$

$$\sigma = \frac{2(.0381)}{\pi(.305)} = .080$$

From simple momentum blade element theory (see Ref. 2) and assuming an ideally twisted blade, one can relate the inflow angle $\lambda = u_p/\Omega R$, the blade drag coefficient C_{Do}, and the power coefficient $C_p = P \,/\, \frac{1}{2}\rho\, V^3\, \pi\, R^2$ for a wind turbine near zero angle of yaw, by the relations,

$$\lambda^2 + \left(\frac{\sigma a}{8} - \frac{V}{\Omega R} \right) \lambda - \frac{\sigma a}{8}\, \theta_o = 0 \tag{A-1}$$

$$C_p = \frac{\sigma a}{4} \left(\frac{\Omega R}{V}\right)^3 \left[2\lambda(\lambda - \theta_o) - \frac{C_{Do}}{a}\right] = 0 \tag{A-2}$$

See Fig. 13 for definitions and directions. For the zero power, free-wheeling condition, one has $C_p = 0$. Equations (A-1) to (A-2) can then be solved to give,

$$\lambda = \left(\frac{\sigma a}{16} - \frac{V}{2\ \Omega R} \right) \pm \sqrt{\left(\frac{\sigma a}{16} - \frac{V}{2\ \Omega R} \right)^2 + \frac{\sigma a}{8}\, \theta_o} \tag{A-3}$$

$$C_{Do} = 2\ a\ \lambda\ (\lambda - \theta_o) \tag{A-4}$$

where the + sign is physically meaningful in Eq. (A-3). Using the previous physical parameters gives,

$\lambda = .1139$

$C_{Do} = .028$

for the equivalent ideally twisted wind turbine used here.

REFERENCES

1. Miller, R.H., "On the Weathervaning of Wind Turbines", J. of Energy, Vol. 3, No. 5, September - October 1979, p. 319-320.

2. Miller, R.H., et al., "Wind Energy Conversion, Vol. 2: Aerodynamics of Horizontal Axis Wind Turbines", M.I.T. Aeroelastic and Structures Research Laboratory Report TR-184-8, U.S. Dept. of Energy Report, COO-4131-T1, (Vol. 2), September 1978.

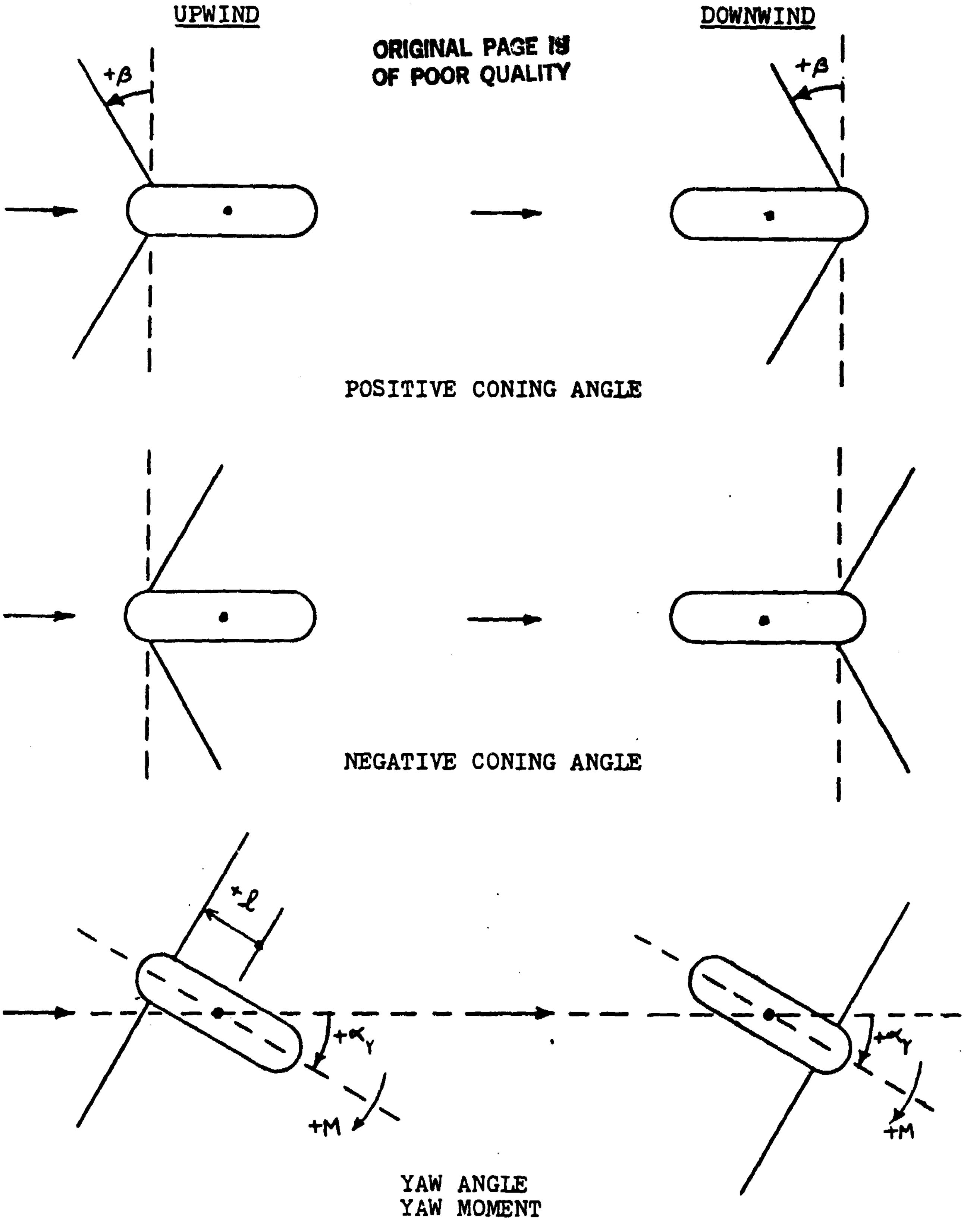

FIG. 1 WIND TURBINE CONFIGURATIONS, TOP VIEW

FIG. 2 PHOTO OF WIND TURBINE AND TURNTABLE

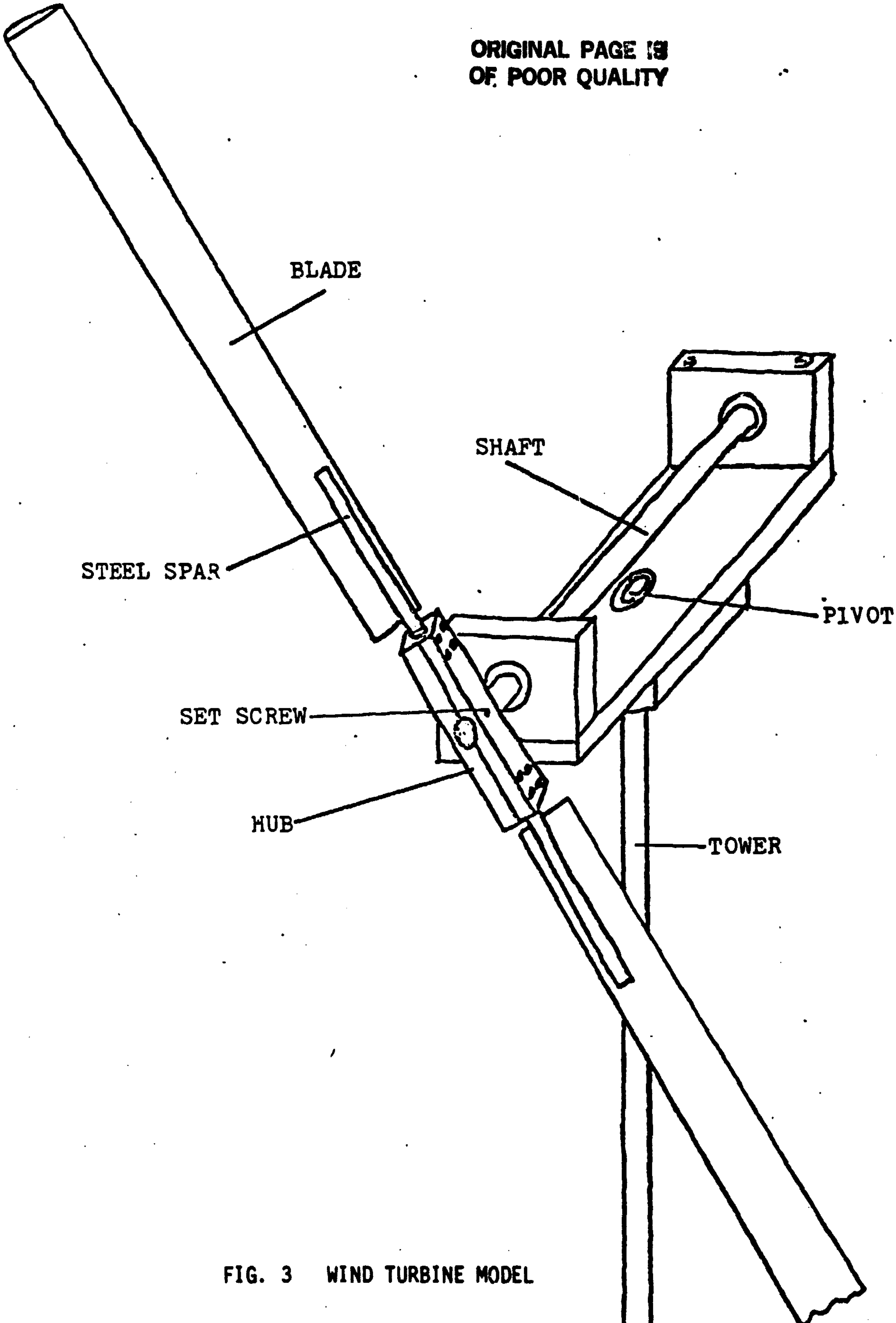

FIG. 3 WIND TURBINE MODEL

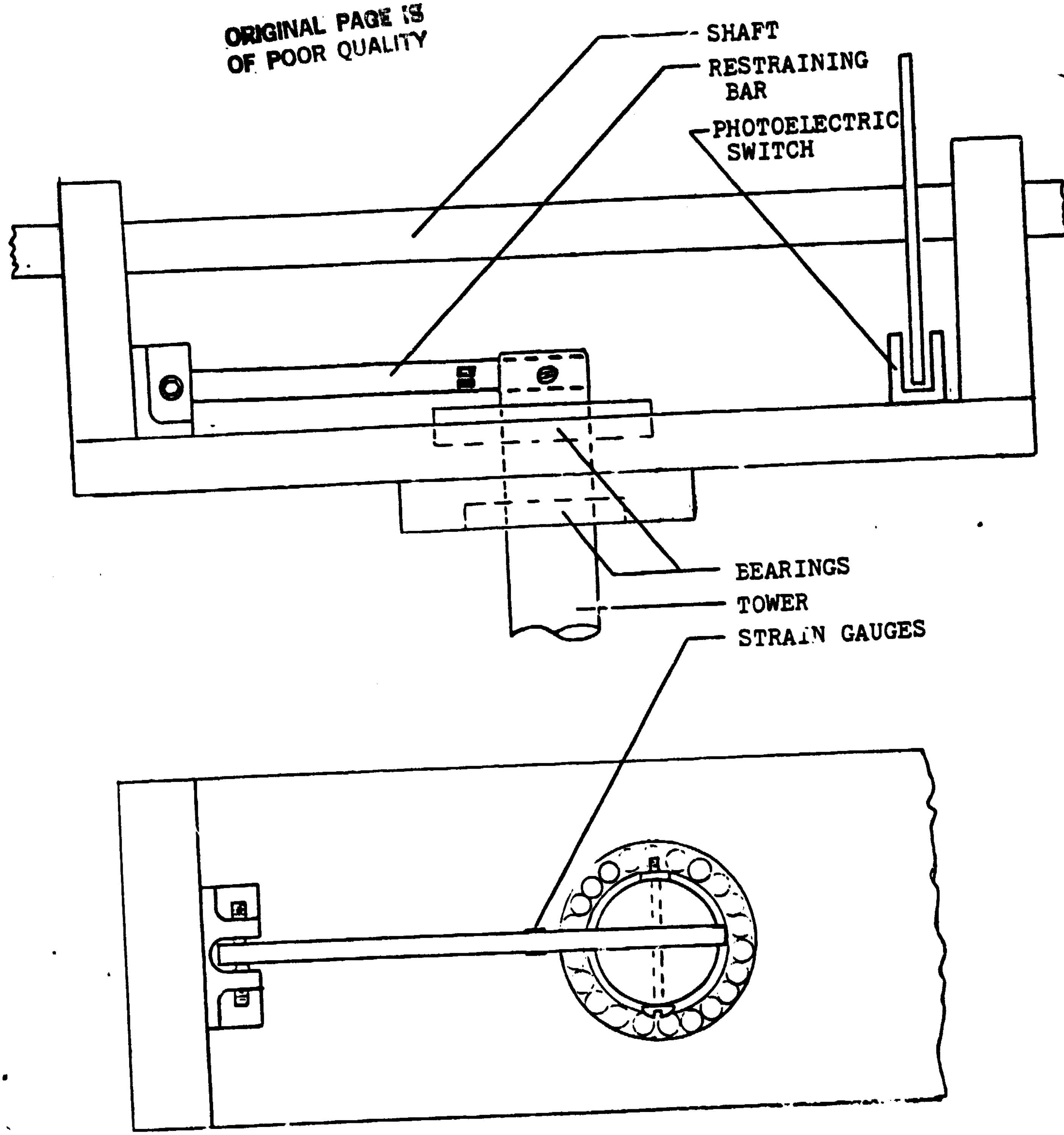

FIG. 4 MEASURING DEVICES

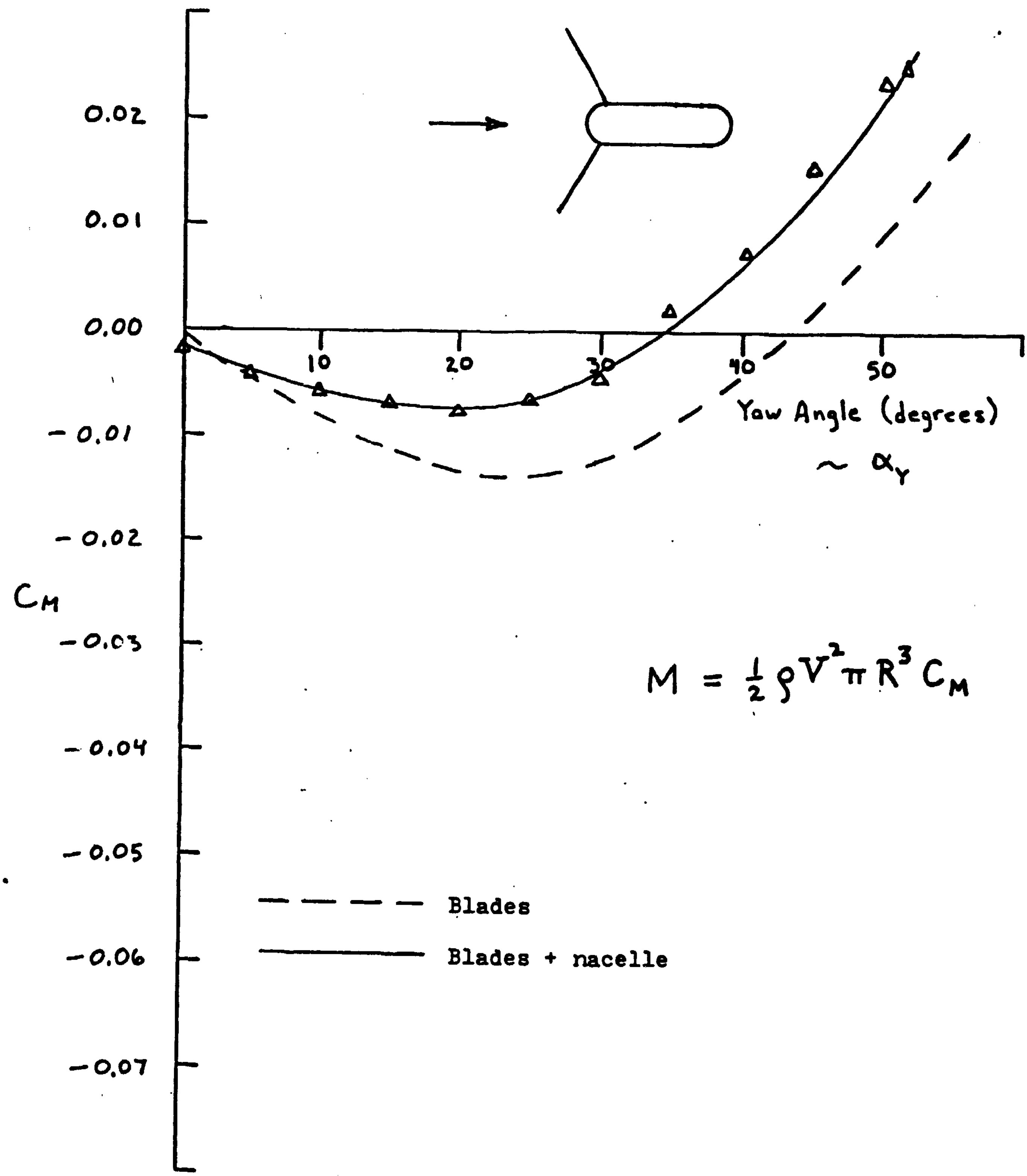

FIG. 5 C_M VS. YAW ANGLE, UPWIND, β = +10°

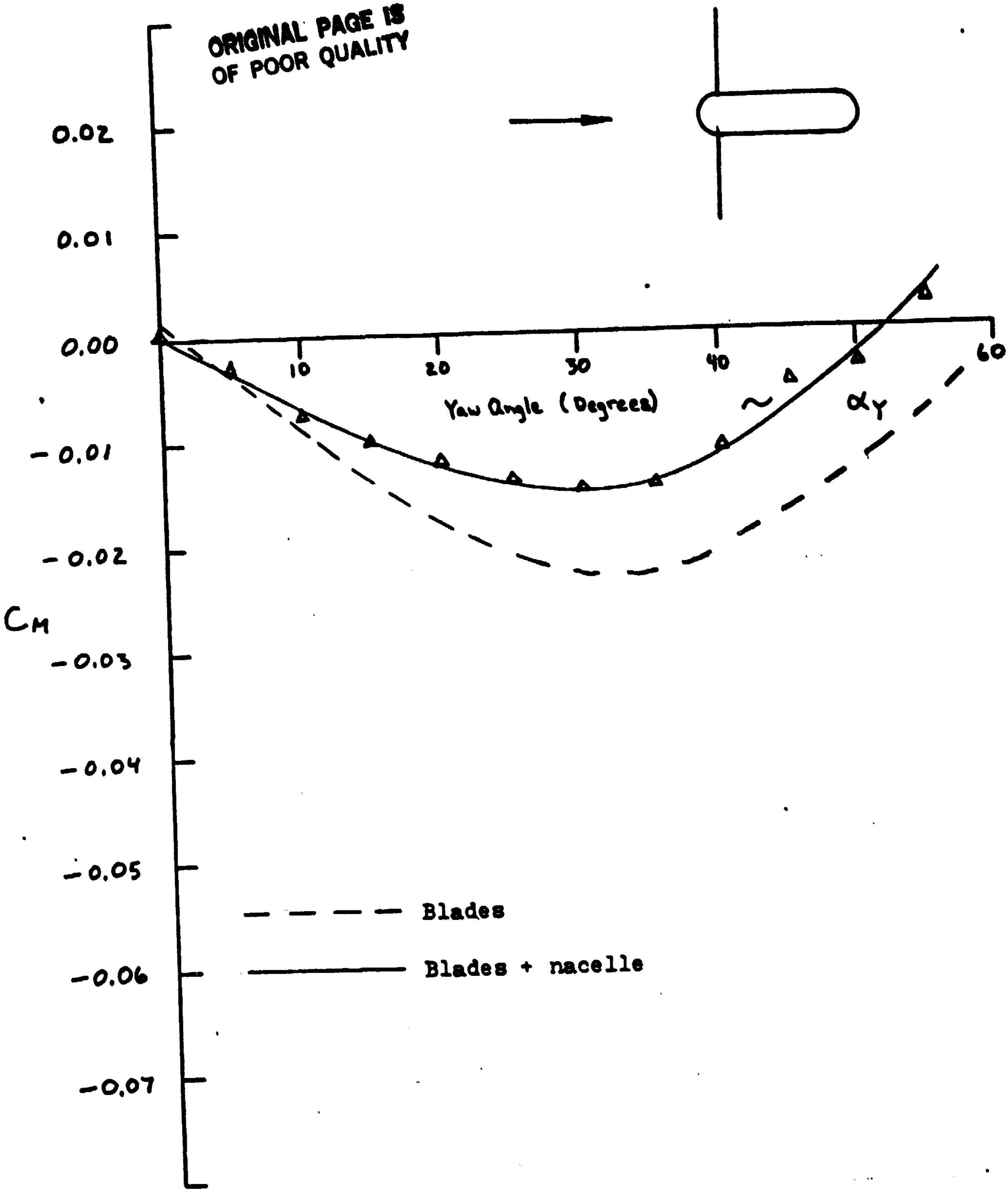

FIG. 6 C_M VS. YAW ANGLE, UPWIND, β = 0°

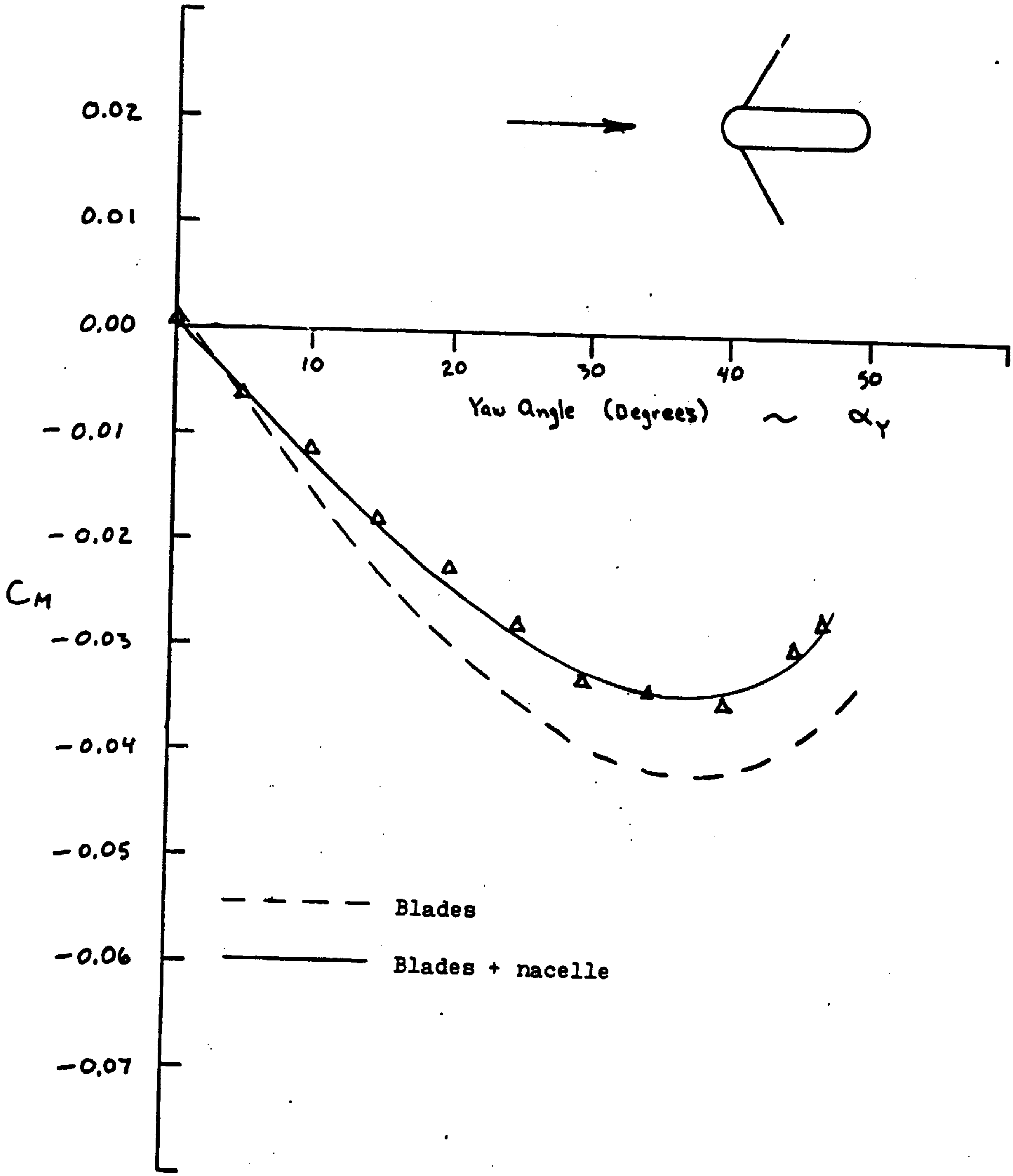

FIG. 7 C_M VS. YAW ANGLE, UPWIND, $\beta = -10°$

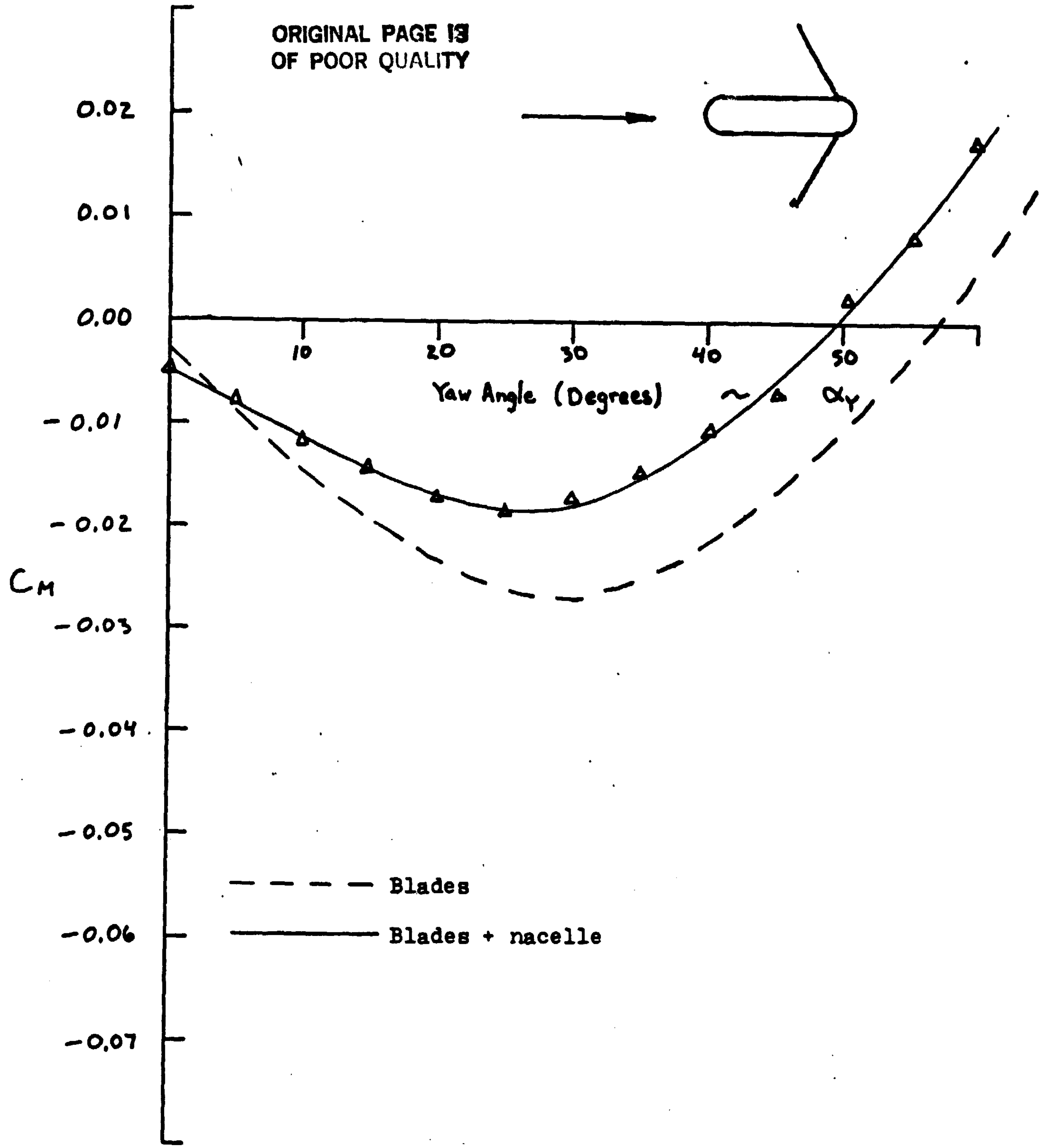

FIG. 8 C_M VS. YAW ANGLE, DOWNWIND, $\beta = +10°$

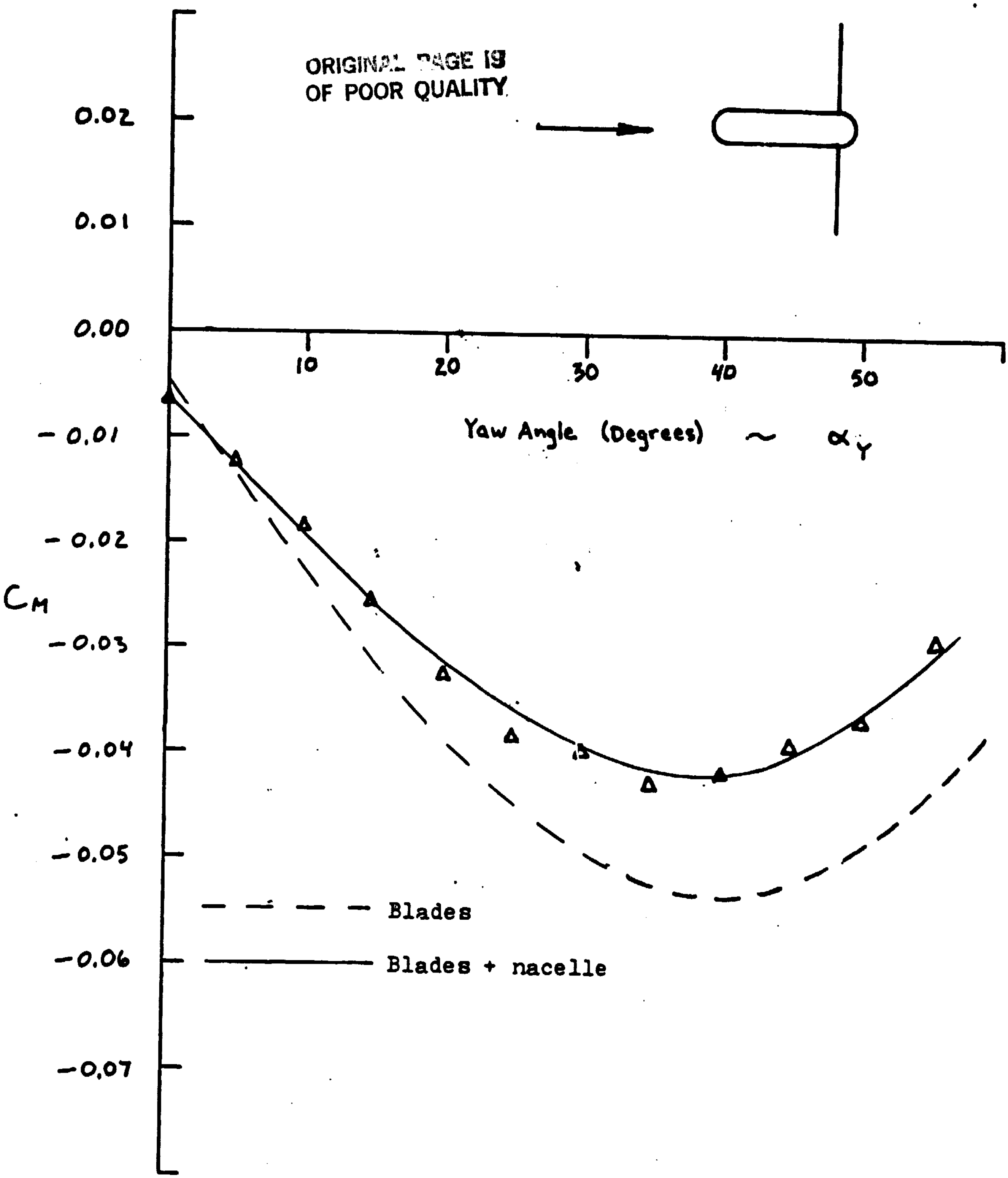

FIG. 9 C_M VS. YAW ANGLE, DOWNWIND, $\beta = 0°$

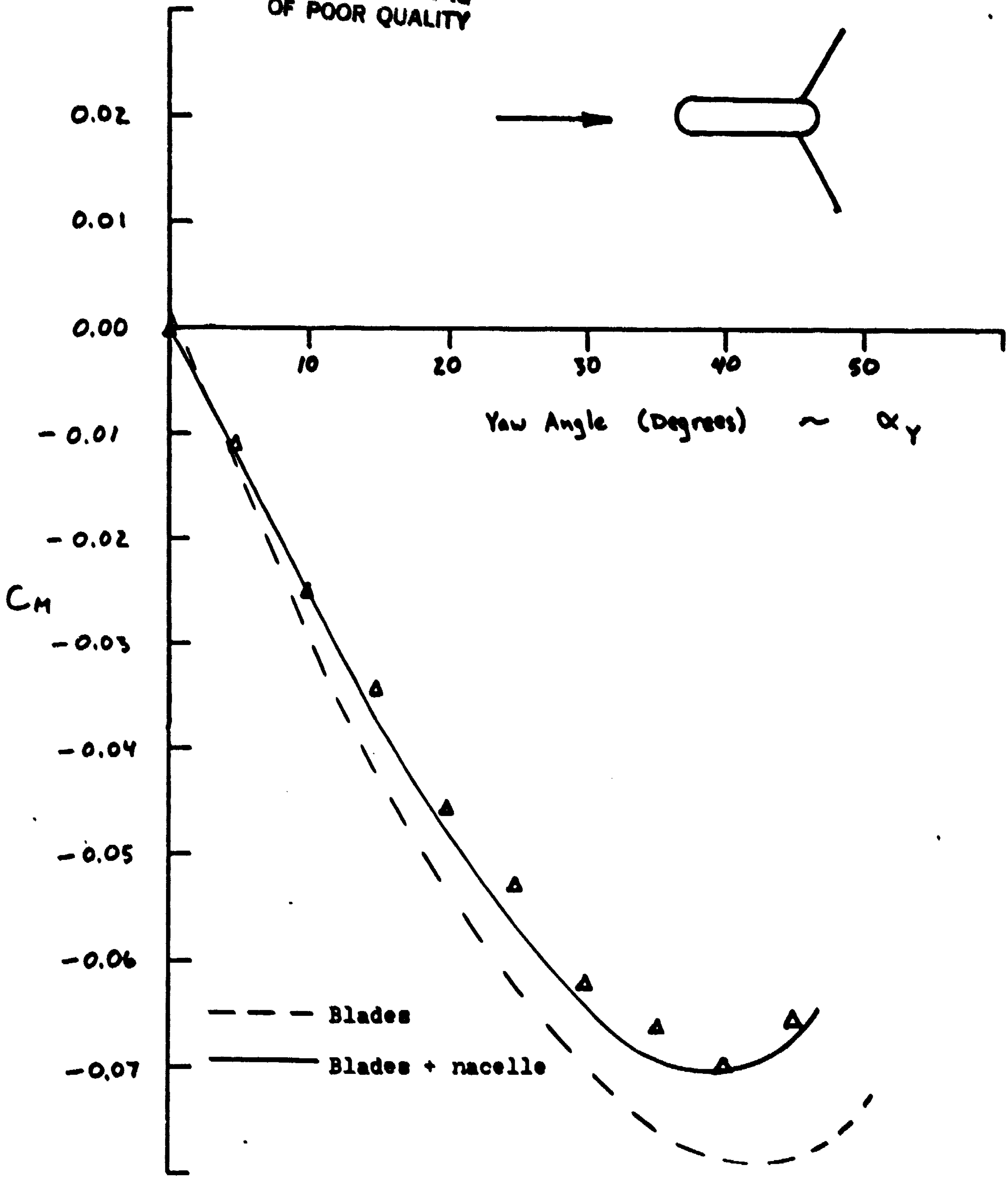

FIG. 10 C_M VS. YAW ANGLE, DOWNWIND, β = -10°

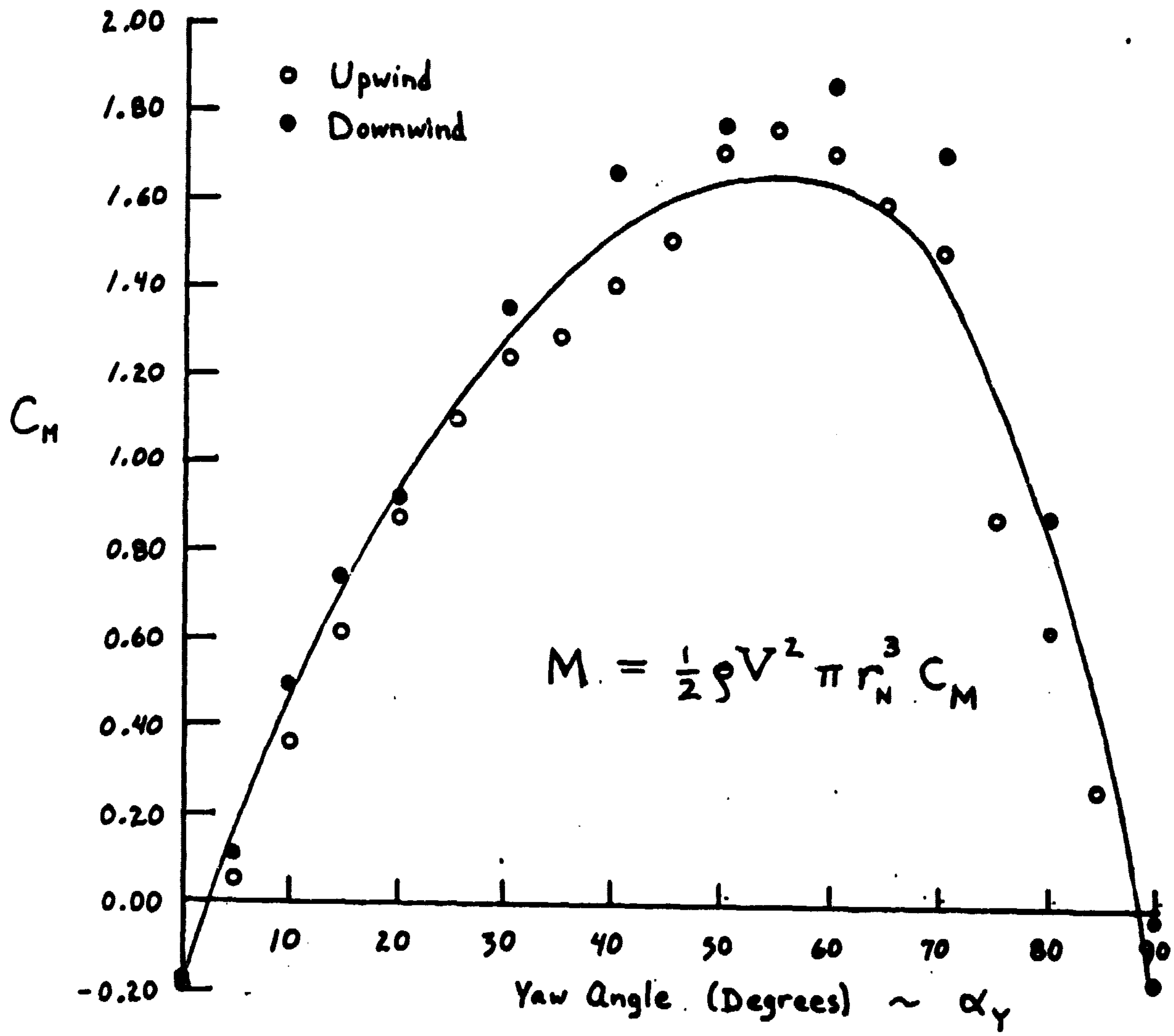

FIG. 11 C_M VS. YAW ANGLE, NACELLE ALONE

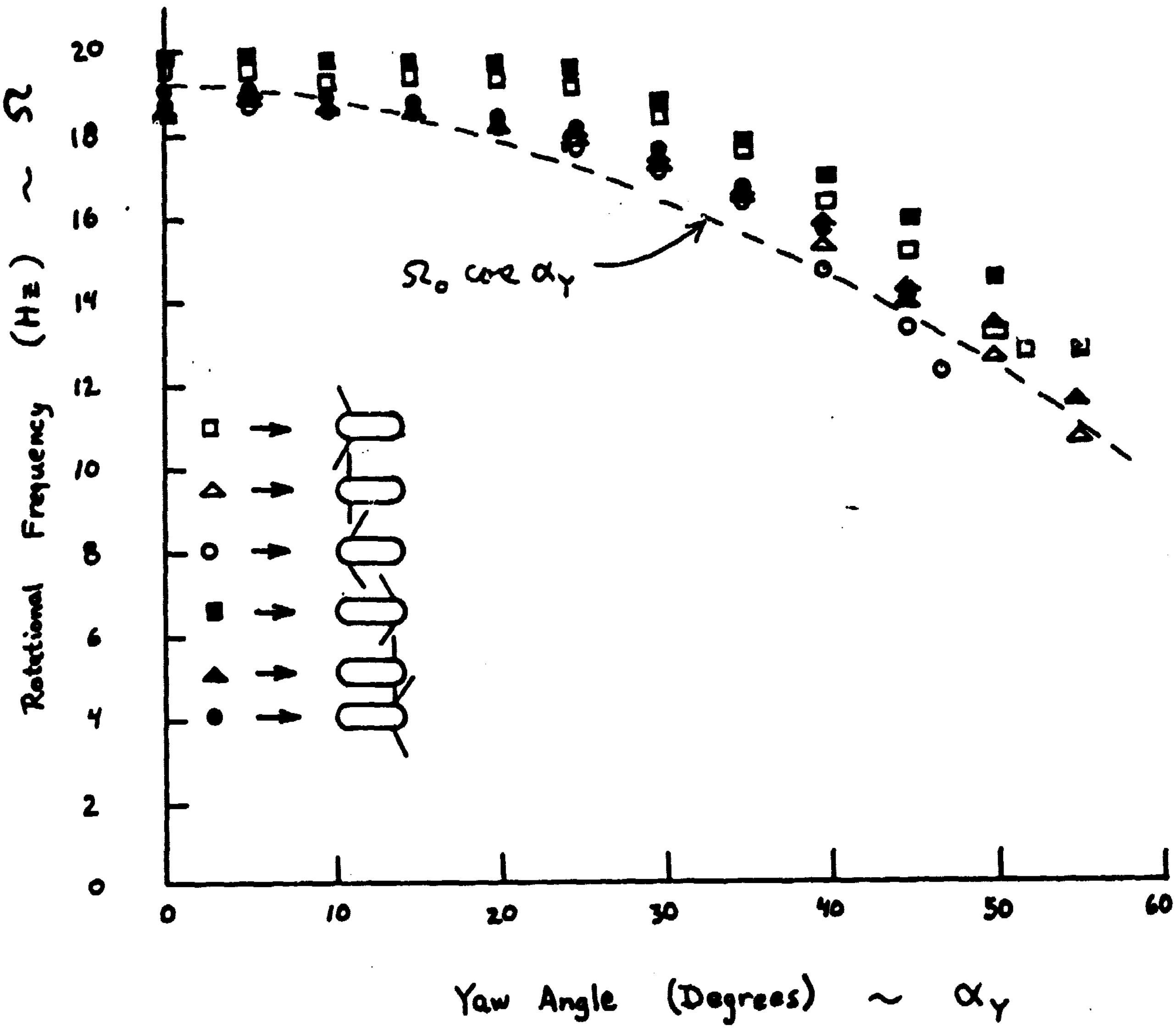

FIG. 12 ROTATIONAL FREQUENCY VS. YAW ANGLE

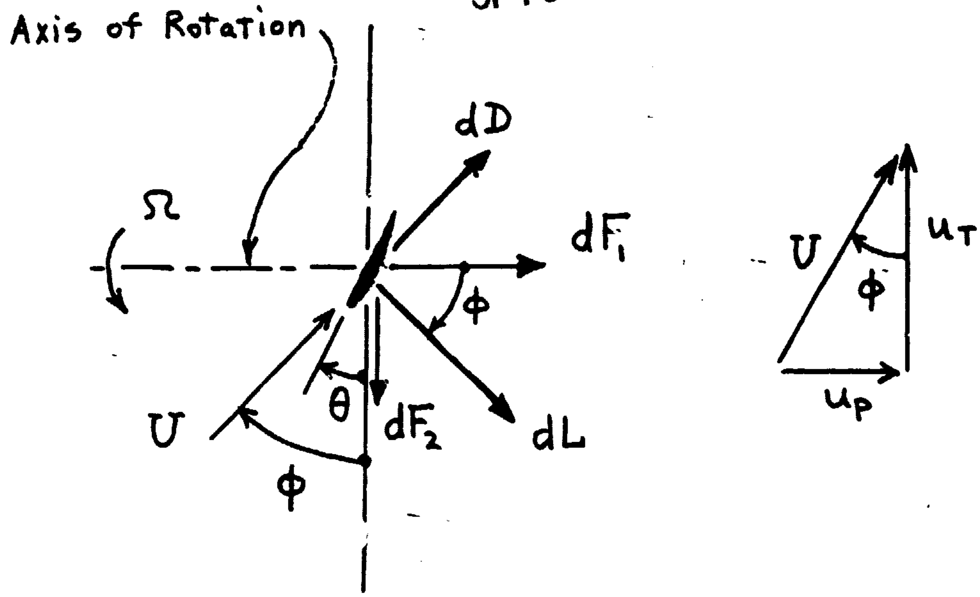

For small angles ϕ,

$$\phi \approx \frac{u_P}{u_T} = \frac{u_P}{\Omega r} = \lambda$$

$$dL = \frac{1}{2}\rho U^2 c\, a(\phi-\theta)\, dr$$

$$dD = \frac{1}{2}\rho U^2 c\, C_{D_0}\, dr$$

FIG. 13 AERODYNAMIC FORCES ON BLADE ELEMENT

TABLE 1. COMPARISON OF MEASURED VALUES OF $\frac{\partial C_M}{\partial \alpha}$ WITH THEORY

	Theory - $\frac{\partial C_M}{\partial \alpha}$ 1 /rad	Measured $\frac{\partial C_M}{\partial \alpha}$ 1 /rad	Measured $\frac{\partial C_M}{\partial \alpha}$ subtracting nacelle effects 1 /rad
Upwind $\beta=+10°$	+0.118	-0.022	-0.045
Upwind $\beta=0°$	+0.016	-0.040	-0.057
Upwind $\beta=-10°$	-0.086	-0.074	-0.091
Downwind $\beta=+10°$	+0.086	-0.034	-0.057
Downwind $\beta=0°$	-0.016	-0.080	-0.097
Downwind $\beta=-10°$	-0.118	-0.148	-0.171